values of $f_p(\epsilon_p)/f_\alpha(\epsilon_\alpha)$, which are given by the ratio of points on the $K=1000$ curve to the corresponding points for $K=0.7$, are seen to be of the order of unity but to depend in detail on the form chosen for the dependence of T on U. Thus, this estimate of the effects due to angular-momentum conservation leaves intact the conclusion that, within experimental error, there is no significant effect of excitation energy on the ratio of reaction cross sections of Co^{59} with proton and with α particles.

It is of interest to note that when it is assumed that the temperature is constant at 1.3 MeV, a reasonable assumption for the excitation energies considered here, the resultant dependence of $f_p(\epsilon_p)/f_\alpha(\epsilon_\alpha)$ on ϵ_α is just of the right form to remove any divergence that may exist between the experimental curves shown in Fig. 2.

PHYSICAL REVIEW VOLUME 163, NUMBER 4 20 NOVEMBER 1967

Neutron Cross Sections of Calcium and Potassium from 2 to 8 MeV*

J. D. Reber† and J. D. Brandenberger
Department of Physics and Astronomy, University of Kentucky, Lexington, Kentucky
(Received 17 July 1967)

Differential cross sections for elastic scattering of neutrons have been measured for calcium at neutron energies of 2.06, 3.29, 5.30, 5.88, 6.52, and 7.91 MeV, and for potassium at neutron energies of 2.06, 3.74, 4.33, 6.52, and 7.91 MeV. The measurements were made using time-of-flight techniques and a liquid-scintillation detector equipped with γ-ray discrimination. Measurements of total cross sections for both nuclei were made between 1.8 and 8.3 MeV. The experimental data were compared to optical-model calculations using the computer code ABACUS-2. Parameter-search procedures produced good fits to the cross sections. The potentials implied for the two nuclei are similar.

INTRODUCTION

THERE have been several recent studies of the scattering of fast neutrons by ^{39}K and ^{40}Ca. The γ-ray de-excitation following fast neutron bombardment has been observed for ^{40}Ca by Day[1] and Tucker[2] and for ^{39}K by Nichols *et al.*[3] The purpose of these investigations was to determine the properties of the low-lying states of ^{40}Ca and ^{39}K, respectively. The neutron elastic differential cross sections of ^{39}K have been measured at 1.49, 2.38, 3.00, and 3.76 MeV by Towle and Gilboy[4] and at 3.7 MeV by Kent *et al.*[5] Towle and Gilboy have also measured the inelastic cross sections to the first three levels of ^{39}K. For ^{40}Ca above 2 MeV the elastic differential cross sections have been measured at 2.0, 3.5, and 6.0 MeV by Seagrave *et al.*,[6] at 3.2 MeV by Becker *et al.*,[7] at 3.7 MeV by Kent *et al.*,[5] and at 4.1 MeV by Vincent *et al.*[6] Recent neutron total cross-section measurements of potassium and calcium have been made by Glasgow and Foster[8] from 3–15 MeV and by Stüwer *et al.*[9] from 4–6 MeV. The measurements of Stüwer *et al.* give values approximately 6% lower than those of Glasgow and Foster.

This study presents precision measurements of the elastic differential cross sections and total cross sections of calcium and potassium between neutron energies of 2 and 8 MeV. This information is useful because of the existing discrepancies in the total cross sections and because it extends the range of information on the neutron elastic scattering by these two nuclei to 7.9 MeV. It the cross sections are represented as scattering by a complex potential, elastic-scattering data over a relatively large energy range is required to determine the energy dependence of the potential parameters. As a part of this study an attempt was made to fit both the calcium and potassium data with optical-model parameters at each energy and to determine the energy dependence of the parameters.

EXPERIMENTAL ARRANGEMENT

The data were taken using the 6-MeV Van de Graaff accelerator of the University of Kentucky. Neutrons of energies up to 5.3 MeV were produced by the $T(p,n)^3He$ reaction and from 5.3–8.3 MeV by the $D(d,n)^3He$

* Work supported in part by the National Science Foundation.
† Present address: Department of Physics, University of Virginia, Charlottesville, Virginia.
[1] R. B. Day, Phys. Rev. **120**, 767 (1956).
[2] W. E. Tucker, Phys. Rev. **140**, B1541 (1965).
[3] Davis B. Nichols and M. T. McEllistrem, submitted to Phys. Rev.
[4] J. H. Towle and W. B. Gilboy, Nucl. Phys. **72**, 515 (1965).
[5] D. W. Kent, S. P. Puri, S. C. Snowdon, and W. P. Bucker, Phys. Rev. **125**, 331 (1962).
[6] M. D. Goldberg, V. M. May, and J. R. Stehn, Brookhaven National Laboratory Report BNL-400, 2nd ed. (unpublished).
[7] R. L. Becker, W. G. Guindon, and G. J. Smith, Nucl. Phys. **89**, 154 (1966).
[8] J. R. Stehn, M. D. Goldberg, B. A. Magurno, and R. Weiner-Chaseman, *Neutron Cross Sections*, Brookhaven National Laboratory Report BNL-325 (U. S. Government Printing Office), 2nd ed., Suppl. No. 2.
[9] D. Stüwer, H. Genz, and M. Borman, Nucl. Phys. **62**, 165 (1965).

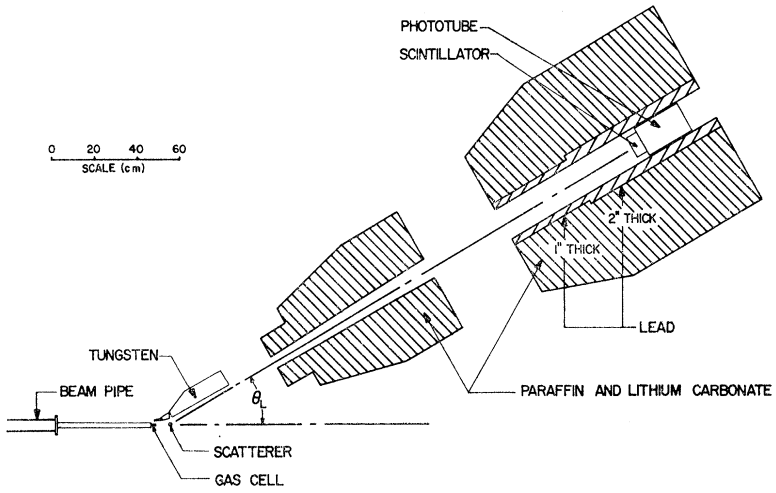

FIG. 1. The experimental arrangement used for the differential cross-section measurements.

reaction. In both cases the beam was pulsed in the terminal and had a pulse width of 5 nsec at a repetition rate of 5 Mc/sec. The tritium and deuterium targets were contained in a gas cell separated from the vacuum side of the beam pipe by a 0.00076-cm thick molybdenum foil.

The samples used for both the total and differential cross sections are described in Table I. The polyethylene sample was used to normalize the differential cross-section measurements to the known cross sections for scattering from hydrogen. To prevent oxidation of the calcium and potassium samples, they were isolated from air. For the total cross-section measurements the calcium sample was coated with a very thin layer of paraffin, and the potassium was contained in a brass cylinder having a wall thickness less than 0.05 cm. For the differential cross-section measurements the calcium was coated with a very thin layer of plastic, and the potassium was contained in a stainless steel cylinder having a wall thickness of 0.007 cm. Identical empty containers of brass and stainless steel were used for background measurements.

Differential Cross Section Measurements

The scattering samples were right cylinders with axes perpendicular to the reaction plane and were suspended 7.6 cm from the center of the gas cell. The neutron detector was between 2 and 3 m from the scatterer in order to give good separation between the elastic and inelastic peaks in a time-of-flight spectrum. Figure 1 shows the shielding arrangement. The detector was contained in a large shield 1 m in diameter by 1.1 m in length filled with a mixture of paraffin and lithium carbonate. A tungsten wedge was used to shield against the direct neutron beam. The complete shielding arrangement was on a carriage which pivoted about the scattering sample.

TABLE I. Samples used for the total and differential cross-section measurements.

Element	Diameter (cm)	Length (cm)	Mass (g)
Samples for Differential Cross Sections			
Ca	2.03	3.86	19.50
K	2.53	4.43	18.93
Polyethylene	0.60	2.53	0.684
Samples for Total Cross Sections			
Ca	2.25	9.59	57.82
K	2.38	9.86	37.27

A liquid scintillator, 4 in. in diam by 2 in. thick, mounted on an Amperex 58 AVP photomultiplier tube was used for neutron detection. The detector had three outputs: a fast timing output, a linear output which was proportional to the detected particle energy, and a pulse-shape discrimination (PSD) output. A PSD pulse was generated only upon the detection of a neutron and, therefore, was used to discriminate against γ rays. Standard time-of-flight (TOF) techniques were used for data collection. The time reference signal was derived from a capacitive pick off in the beam pipe. The output signal from a time to amplitude converter was fed into a multichannel analyzer. Coincident pulses from the PSD and linear outputs were required to gate the analyzer. With this arrangement over 90% of the γ rays were rejected with the neutron detection threshold at 400 keV. The neutron flux monitor was a small plastic scintillator situated directly above the gas cell. Its counting rate was gated with TOF techniques to discriminate against neutrons not coming directly from the gas cell.

Below 5.3 MeV, where the $T(p,n)^3He$ reaction was used, the signal to background ratio was better than 10 to 1. However, at higher energies where deuterons were used, the neutron background increased appreciably. For the worst case (7.92-MeV neutrons), the signal to background ratio was 2 to 1 at 90°. Data were taken at various angles between 25° and 150°. Two time spectra were taken at each angle: one with the sample in place, and one with the sample removed

which was then subtracted from the sample spectrum. Figure 2 shows a typical time spectrum with background subtracted.

Total Cross Section Measurements

The total cross sections were measured by the transmission method. The neutron detector was a 1-in. diam by 1-in. thick plastic scintillator mounted on a RCA 6810A photomultiplier tube. The electronics were similar to those used for the differential cross-section measurements with the exception that no PSD pulse was used. The detector was at 0° with respect to the accelerated beam and about 250 cm from the neutron source. The samples were located 70 cm from the neutron source.

ANALYSIS AND CROSS SECTIONS

The measured total cross sections for potassium (93.1% ^{39}K) and calcium (96.97% ^{40}Ca) are shown by the points in Fig. 3. The energy spread of the neutron flux varied from 50 keV at 2 MeV to 35 keV at 5.3 MeV where the tritium target was used and from 140 keV at 5.3 MeV to 95 keV at 8.3 MeV where the deuterium target was used. The error bars shown for a number of points in Fig. 3 represent the standard error arising from statistical uncertainties, neutron monitoring uncertainties, background subtraction uncertainties, and uncertainties due to finite geometry. Corrections were made for the dead time of the counting electronics, and for in scattering by the method of Bratenahl *et al.*[10] Deadtimes were typically 3% and inscattering, based on the measured elastic differential cross section, was less than 0.3%. Since the time-of-flight technique was used, no neutrons inelastically scattered into the detector were counted. Analysis of repeated measurements indicate that the stated errors are reasonable.

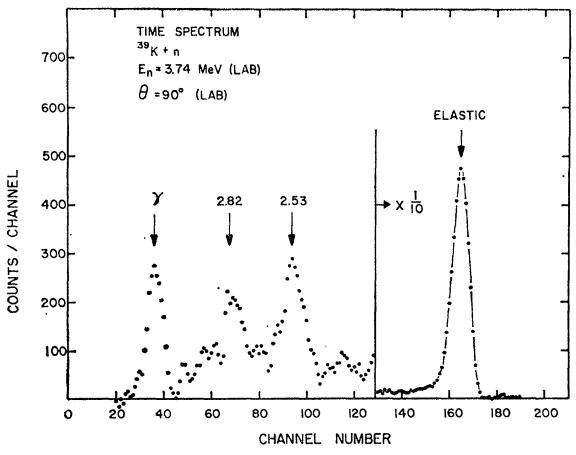

FIG. 2. Time-of-flight spectrum taken at 90° for 3.74 MeV neutrons scattered from potassium. The background has been subtracted. The flight path was 2.02 m, and the time calibration is 0.88 nsec/channel.

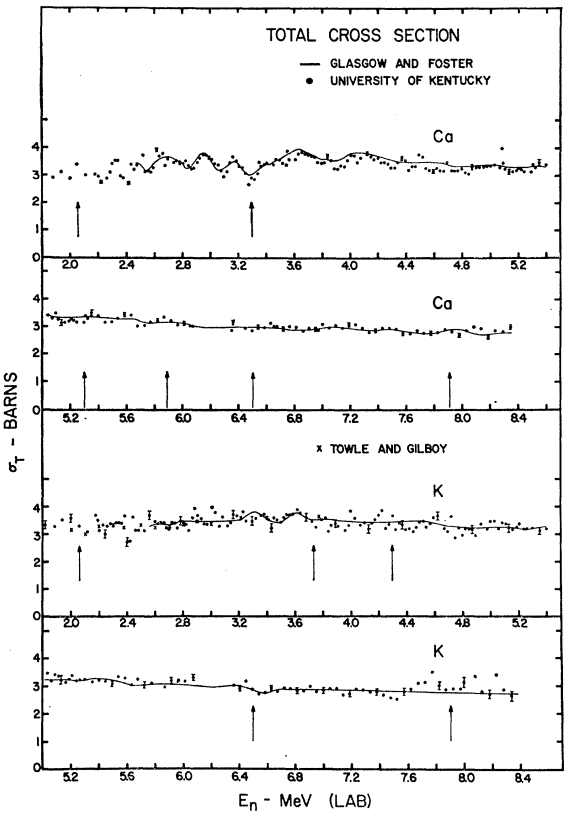

FIG. 3. Total neutron cross sections of calcium and potassium. The arrows indicate where differential cross sections were measured.

Several groups have recently reported total cross-section measurements in the 2- to 8-MeV energy range. The measurements of Stüwer *et al.*[9] do not agree well with those of Glasgow and Foster,[8] the former getting values about 6% lower. The reported values of Glasgow and Foster have an error of about 1% in the energy scale.[11] Their measurements with the energy correction are shown in Fig. 3. It is seen that there is good agreement in detail between their results and the present measurements. Also, for potassium between 2 and 4 MeV there is good agreement with the measurements of Towle and Gilboy.[4]

The calcium total cross sections show a considerable amount of structure, especially below 3.6 MeV where the cross section varies between 2.6 and 3.8 b with successive maxima and minima about 200 keV apart. This structure is significant in interpreting cross sections calculated by the optical model. Specifically, in a region of fluctuations, only suitably averaged measurements can be expected to give good agreement with optical-model calculations.

The differential cross sections have been measured for potassium and calcium at the energies indicated by the

[10] A. Bratenahl, J. M. Peterson, and J. P. Stoering, Phys. Rev. **110**, 927 (1958).

[11] D. G. Foster, Jr. (private communication).

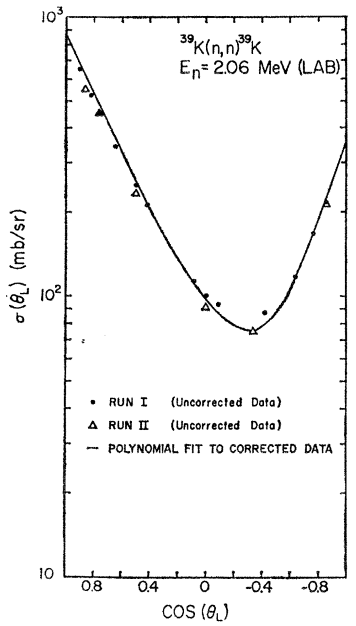

FIG. 4. Elastic differential cross section for 2.06-MeV neutrons scattered from potassium. This shows the reproducibility of the data. The solid curve is a least-squares fit of the corrected data to a series of Legendre polynomials.

arrows in Fig. 3. The angular distributions were normalized by comparison with neutron-proton scattering at 40° in the laboratory system using a polyethylene scatterer. Figure 4 shows uncorrected differential cross sections for potassium taken at 2.06-MeV neutron energy. The two sets of data points in Fig. 4 represent two completely independent measurements taken several months apart.

The differential cross sections were corrected for dead time of the counting electronics, angular resolution, flux attenuation, and multiple scattering in the sample. The correction for angular resolution (±7.6° max for Ca, ±9.4° max for K) was less than 7% for calcium and less than 12% for potassium. Corrections for the effect of attenuation of neutrons, both on entering and leaving the sample, were made using the method of Cranberg[12] and amounted to less than 10% for calcium and less than 7% for potassium. This correction was applied to the integrated differential cross section and, therefore, represents an average correction to the data points. Multiple-scattering corrections to the angular distributions were made using the method introduced by Walt.[13,14] These corrections are described in detail elsewhere.[15] The corrections amounted to less than 3.5% at 30° and less than 16% at 90°. The effect of all the above corrections on the differential cross sections for potassium at 2.06 MeV neutron energy is illustrated in Fig. 4. The solid curve is the Legendre polynomial fit to the corrected experimental data.

The relative errors assigned to the angular distributions are due to counting statistics, extraction of yields from time-of-flight spectra, reproducibility of sample position and angular settings, neutron monitor instabilities, and the previously mentioned data corrections. Statistical uncertainties were typically 2% but were as high as 7% where the cross section values were less than 10 mb/sr. All other uncertainties entering into the relative errors totaled less than ±3%. At least two data points per angular distribution were repeated at the end of each angular-distribution measurement to check reproducibility.

Errors in the absolute cross sections arise from the relative errors and from the neutron-proton scattering normalization.

A knowledge of the efficiency of the detector as a function of neutron energy was necessary to complete the normalization. The detector's relative efficiency was measured over the energy region of 0.5–8.3 MeV.

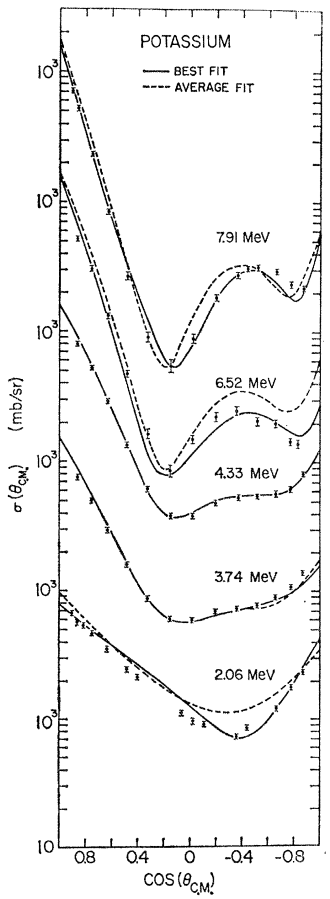

FIG. 5. Optical-model fits to the elastic differential cross sections of calcium. The solid curves are the best fits; the parameters are listed in Table V. The dashed curves were calculated using an average set of parameters (V=50 MeV, W=6 MeV, and U=6 MeV).

[12] L. Cranberg, Los Alamos Scientific Laboratory Report No. LA-2177, 1959 (unpublished).
[13] M. Walt and H. H. Barschall, Phys. Rev. 93, 1062 (1954).
[14] M. Walt, Ph.D. dissertation, University of Wisconsin, 1953 (unpublished).
[15] J. D. Reber, Ph.D. dissertation, University of Kentucky, 1967 (unpublished).

TABLE II. Elastic differential cross-section measurements of calcium. The uncertainties are the total root-mean-square uncertainties. Cos(θ) and $\sigma(\theta)$ are in center-of-mass system. All cross sections are in mb/sr.

Cos(θ)	E_n=2.06 MeV ΔE_n=115 keV $\sigma(\theta)$	E_n=3.29 MeV ΔE_n=95 keV $\sigma(\theta)$	E_n=5.30 MeV ΔE_n=245 keV $\sigma(\theta)$	E_n=5.88 MeV ΔE_n=205 keV $\sigma(\theta)$	E_n=6.52 MeV ΔE_n=160 keV $\sigma(\theta)$	E_n=7.91 MeV ΔE_n=220 keV $\sigma(\theta)$
0.902	775 ±38					855 ±41
0.860		699 ±34	733 ±37	729 ±36	649 ±32	639 ±30
0.811	554 ±27					
0.755	466 ±22	437 ±21	446 ±22	383 ±19	323 ±16	257 ±11.5
0.694	404 ±19		326 ±16			
0.628	334 ±16	279 ±13	192 ± 9.1	186 ± 9.2	152 ± 9.0	86.6± 4.4
0.557			149 ± 7.2			
0.481	218 ±10	155 ± 9.1	75.5± 3.7	71.9± 4.1	38.5± 3.0	23.0± 1.6
0.402	189 ± 8.8		53.6± 2.9			
0.320	157 ± 7.2	94.9± 4.6	27.5± 1.9		13.0± 1.3	9.0± 0.79
0.235			22.6± 1.6	10.9± 1.3		
0.149	117 ± 5.3	73.8± 4.1	19.7± 1.4	11.7± 1.3	10.3± 1.0	6.4± 0.58
0.062	107 ± 4.9		23.1± 1.4			
−0.025	97.8± 4.6	77.1± 3.8	27.8± 1.6	20.7± 1.6	17.0± 1.4	10.9± 0.8
−0.112	91.4± 4.2					
−0.198	92.6± 4.2	77.6± 4.6	36.5± 2.1	25.8± 2.0	25.9± 2.1	20.8± 1.1
−0.282				31.9± 2.5		
−0.364	100 ± 4.5	85.0± 5.4	38.2± 2.1	33.7± 2.7	35.7± 3.1	31.4± 1.6
−0.443	108 ± 4.9					32.6± 1.6
−0.519	121 ± 5.5	89.7± 4.3	44.4± 2.4	36.7± 3.0	27.2± 2.4	35.8± 1.8
−0.657	173 ± 7.8	102 ± 4.9	38.3± 2.4		23.4± 2.1	29.8± 1.5
−0.720	194 ± 9.0			31.7± 2.1		
−0.776	244 ±11	137 ± 7.0	44.6± 2.4	33.4± 2.1	26.0± 2.3	26.2± 1.4
−0.827					21.9± 2.0	
−0.872	334 ±16	188 ± 9.1	51.8± 2.8	29.5± 1.8		23.4± 1.2

The root-mean-square uncertainty, exclusive of the statistical and multiple scattering errors, since these are different for each differential cross-section point, is ±4.5%. Figures 5 and 6 show the corrected differential cross sections of potassium and calcium in the center-of-mass system. Note that the error bars shown are total root-mean-square errors, not relative errors. Tables II and III list the differential cross sections and their total root-mean-square errors.

Legendre polynomial fits to the corrected data were calculated using a computer program, which determined the polynomial coefficients and their uncertainties based on the theory of least-squares curve fitting of Cziffra and Moravcsik.[16] The coefficients were determined by the smallest χ^2 fit of the data. The order of the Legendre polynomial expansion was determined by three criteria: (1) The χ^2 fit was not significantly improved by including higher order polynomials, (2) the

TABLE III. Elastic differential cross-section measurements of potassium. The uncertainties are the total root-mean-square uncertainties. Cos(θ) and $\sigma(\theta)$ are in the center-of-mass system. All cross sections are in mb/sr.

Cos(θ)	E_n=2.06 MeV ΔE_n=115 keV $\sigma(\theta)$	E_n=3.74 MeV ΔE_n=85 keV $\sigma(\theta)$	E_n=4.33 MeV ΔE_n=78 keV $\sigma(\theta)$	E_n=6.52 MeV ΔE_n=160 keV $\sigma(\theta)$	E_n=7.91 MeV ΔE_n=220 keV $\sigma(\theta)$
0.902	675 ±32				716 ±34
0.859	568 ±27	751 ±36	802 ±38	516 ±24	524 ±24
0.811	541 ±26				
0.755	467 ±22	504 ±24	522 ±24	305 ±15	236 ±11
0.627	355 ±17	295 ±13	293 ±13	133 ± 6.7	84.4± 4.3
0.480	246 ±11	160 ± 7.2	136 ± 6.1	47.5± 3.0	27.3± 1.9
0.401	216 ±10				
0.319		87.1± 4.0	62.0± 3.2	16.6± 1.5	9.2± 0.8
0.149		60.7± 2.9	38.6± 2.1	8.6± 0.9	5.5± 0.7
0.061	112 ± 5.2				
−0.026	95.8± 4.5	59.5± 2.7	38.8± 1.9	15.2± 1.2	9.0± 0.8
−0.113	91.8± 4.3				
−0.199		69.9± 3.2	49.5± 2.4	22.6± 1.8	18.5± 1.2
−0.365	73.1± 3.5	73.5± 3.3	53.6± 2.5	25.1± 2.0	27.6± 1.6
−0.444	85.9± 4.1				30.9± 1.6
−0.519		77.5± 3.5	55.5± 2.6	20.9± 1.7	31.6± 1.6
−0.658	121 ± 5.6	89.3± 4.0	58.2± 2.7	20.3± 1.7	29.5± 1.5
−0.777	179 ± 8.2	108 ± 4.8	61.8± 2.8	14.5± 1.2	23.4± 1.2
−0.828				14.0± 1.2	
−0.872	237 ±11	140 ± 6.3	82.1± 3.8		21.9± 1.2

[16] P. Cziffra and M. J. Moravcsik, University of California Radiation Laboratory Report No. UCRL-8523 Rw., 1959 (unpublished).

TABLE IV. Legendre polynomial coefficients of least-squares fits to the data of Tables II and III. The expansion is given by: $W(\theta)=\sum A_L P_L(\cos\theta)$. A_L's are in mb/sr; energies are in MeV.

Coeff. \ E_n	2.06	3.29	3.74	4.33	5.30	5.88	6.52	7.91
				Calcium				
A_0	257.2± 1.9	212.2± 2.8			162.9± 4.7	157.8± 4.7	132.2± 4.0	128.9± 2.3
A_1	181.6± 5.9	236.1± 6.5			311.6±11.7	328.2±10.3	272.5± 7.9	282.9± 5.2
A_2	399.6± 7.2	378.6±11.4			396.9±18.4	423.8±19.6	360.8±16.5	390.8± 9.8
A_3	82.2±10.7	185.3±11.2			307.0±17.7	361.1±18.8	304.9±13.6	383.3± 9.7
A_4	127.3± 9.3	151.5±14.8			177.5±19.2	237.4±26.8	204.3±21.3	281.1±13.4
A_5	20.4±11.4	13.3±10.2			51.5±11.8	115.5±20.3	72.6±12.3	173.2± 9.9
A_6	19.7± 6.9	17.9±10.6			15.7±11.2	73.7±24.0	37.7±15.9	100.2±11.9
A_7	8.4± 8.2					30.4±12.0		33.6± 6.2
A_8						23.8±12.7		6.9± 6.9
				Potassium				
A_0	230.5± 2.1		209.1±1.2	194.5±1.5			106.6± 2.2	110.5± 0.4
A_1	203.6± 4.4		285.3±2.8	333.5±3.6			225.6± 5.1	234.3± 0.8
A_2	302.1± 6.3		389.6±4.7	413.4±6.1			271.9± 9.1	323.5± 1.6
A_3	32.6± 6.4		219.1±4.8	273.1±6.1			228.1± 8.3	305.9± 1.5
A_4	61.1± 7.3		125.9±5.9	142.2±7.5			127.3±11.0	217.4± 2.2
A_5			8.7±4.0	18.5±5.2			40.6± 6.4	126.9± 1.6
A_6			5.2±4.0	8.1±5.2			13.2± 6.9	77.0± 2.0
A_7								22.6± 1.0
A_8								7.5± 1.1

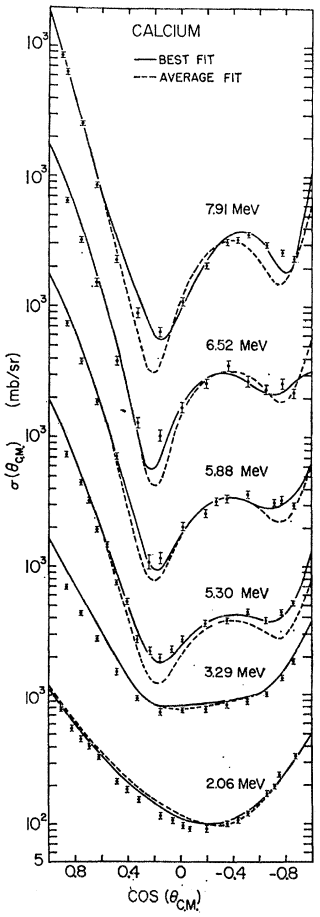

FIG. 6. Optical-model fits to the elastic differential cross sections of potassium. The solid and dashed curves are described in the caption of Fig. 5.

next-higher-order coefficient was smaller than its uncertainty, and (3) the addition of higher-order polynomials did not change the integrated cross section by an amount greater than its uncertainty. These polynomial coefficients and their uncertainties are listed in Table IV.

Several researchers have recently measured differential cross sections of potassium and calcium in this energy region. Since most of these measurements were

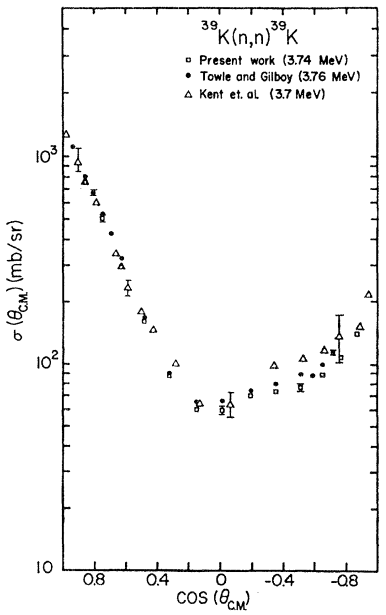

FIG. 7. Elastic differential cross section for 3.74-MeV neutrons scattered from potassium. Comparison is made with Kent *et al.* at 3.7 MeV and with Towle and Gilboy at 3.76 MeV.

made at energies different from the ones presented here, comparisons cannot be made. However, for potassium at 3.74 MeV direct comparison can be made with Kent *et al.*,[5] whose measurements are at 3.7 MeV and with Towle and Gilboy,[4] whose measurements are at 3.76 MeV. These are shown in Fig. 7. Within the experimental errors there is good agreement among the three sets of measurements. Direct comparison can also be made for calcium at 2.06 MeV with the measurements of Seagrave *et al.*[6] at 2.0 MeV. The agreement between the shapes of the two sets of measurements is not good. However, this is not surprising, since in this energy region the total cross section shows considerable fluctuation, the differential cross section can change considerably with an energy change of 60 keV. For calcium at 3.29 MeV comparison can be made with the measurements of Becker *et al.*[7] at 3.2 MeV. Our measurements are more isotropic. This difference in the two curves, as in the case at 2.06 MeV, might be attributed to the change in the cross section as a function of energy.

THEORETICAL ANALYSIS

Theoretical calculations of the elastic differential cross sections of calcium and potassium, using the optical model, were made with the aid of the ABACUS-2 computer code.[17] The complex potential used in the optical-model calculations was of the form

$$V(r)=-V\left[1+\exp\left(\frac{r-R}{a}\right)\right]^{-1}$$
$$-i4a'W\frac{d}{dr}\left[1+\exp\left(\frac{r-R'}{a'}\right)\right]^{-1}$$
$$-\left(\frac{\hbar}{m_\pi c}\right)^2\frac{U}{r}\frac{d}{dr}\left[1+\exp\left(\frac{r-R}{a}\right)\right]^{-1}\mathbf{l}\cdot\boldsymbol{\sigma},$$

where $R=r_0A^{1/3}$ and $R'=r_0'A^{1/3}$. The optical model predicts only the shape-elastic cross sections, whereas the measured elastic differential cross sections include both shape-elastic and compound-elastic contributions. The compound-elastic contributions were calculated using the Hauser-Feshbach theory, where the transmission coefficients were determined from the complex potential.

[17] E. H. Auerbach, Brookhaven National Laboratory Report No. BNL 6562, 1962 (unpublished).

TABLE V. Optical-model parameters and cross sections obtained from fitting the differential cross sections. Energies and potentials are in MeV; cross sections are in barns.

E_n	σ_T Calc	σ_T Exp	σ_{El} Calc	σ_{El} Exp	V	W	U	χ^2 Best fit	χ^2 Average fit
				Calcium					
2.06	3.46	3.30	3.46	3.23	51	7	0	5.33	10.15
3.29	3.77	2.93	3.33	2.67	51	6	2	15.12	16.04
5.30	3.50	3.35	2.45	2.05	49	4	6	6.57	15.00
5.88	3.24	3.25	2.15	1.98	49	5	7	4.13	6.71
6.52	3.06	3.00	1.96	1.66	50	6	8	6.36	6.65
7.91	2.78	2.90	1.65	1.62	48	5	4	7.43	15.88
				Potassium					
2.06	3.17	3.31	3.16	2.90	50	3	0	11.49	37.65
3.74	3.69	3.35	2.90	2.63	50	6	8	4.51	5.05
4.33	3.56	3.40	2.61	2.44	50	6	6	0.91	0.91
6.52	2.91	2.82	1.65	1.34	49	10	6	6.64	32.87
7.91	2.65	2.85	1.49	1.39	48	7	5	4.97	16.07

The values of r_0, r_0', a, and a' were fixed throughout the analysis at 1.25, 1.30, 0.65, and 0.47 F, respectively. At each energy where the differential cross section was measured the three potential strengths were varied to obtain a minimum χ^2 fit to the data.

The optical-model parameters which resulted in the best agreement (by the χ^2 test) with the experimental results are listed in Table V. The calculated differential cross sections are shown by the solid curves in Figs. 5 and 6.

Cross sections were calculated with the set of average parameters of Table V and are shown by the dashed curves in Figs. 5 and 6. In cases where no dashed curves appear, the two calculations are too nearly identical to show as separate curves. The resulting values of χ^2 are listed in Table V.

As seen in Table V the parameters for the two nuclei show slight differences, but it would require a more exhaustive study to show that these differences are actually significant. Further, it is clear that there is no significant change in the parameters with neutron energy between 2 and 8 MeV. The fact that the fits are not uniformly good at all energies indicates that the oversimplified model used in the calculations cannot fully describe the scattering of neutrons by calcium and potassium.

ACKNOWLEDGMENTS

The authors wish to thank Professor M. T. McEllistrem and the University of Kentucky Computing Center for their assistance.